



High-Resolution Ultrasound Elasticity Imaging to Evaluate Dialysis Fistula Stenosis

William F. Weitzel,* Kang Kim,†† Dae Woo Park,*† James Hamilton,§
Matthew O'Donnell,¶ Thomas J. Cichonski,* and Jonathan M. Rubin**

Departments of *Internal Medicine and †Biomedical Engineering, University of Michigan, Ann Arbor, Michigan, ‡Cardiovascular Institute, School of Medicine, University of Pittsburgh, Pittsburgh, Pennsylvania, §Pixel-Velocity, Inc., Ann Arbor, Michigan, ¶Department of Bioengineering, University of Washington, Seattle, Washington, and **Department of Radiology, University of Michigan, Ann Arbor, Michigan

ABSTRACT

Accurate, noninvasive characterization of arterial wall mechanics and detection of fibrotic vascular lesions could vastly improve the ability to predict patient response to local treatments such as angioplasty. Current imaging and other techniques for determining wall compliance rely on imprecise or indirect estimates of wall motion. This study used high-resolution ultrasound imaging with phase-sensitive speckle tracking to obtain detailed and direct measurements of arterial

stiffness in two subjects with dialysis fistula dysfunction. In both subjects, the absolute values of strain were much higher in normal regions of fistula than in regions of stenosis. The lower values of strain in stenotic fistula indicate greater stiffness of the vessel wall. The ultrasound speckle tracking technique used here may have potential to determine vascular mechanical properties noninvasively with a level of precision and accuracy not currently available.

Elasticity imaging has the potential for high-resolution noninvasive monitoring and characterization of vascular pathologies by measuring mechanical properties. Previous attempts at noninvasive vascular elasticity imaging include arterial wall-motion estimation (1–4), intraparietal strain imaging (5), and pulse-wave velocity measurement (6,7). Arterial compliance measurement has also been conducted by monitoring internal pulsatile deformation in tissues surrounding the normal brachial artery (8). Within limits, these measurements have correlated with clinical events, including stroke (9) and claudication symptoms (2) in non-end-stage renal disease (ESRD) patients and adverse cardiovascular events in patients with ESRD (10,11), as well as length of time on dialysis (3). However, current imaging modalities and noninvasive methods of compliance measurement are limited in that they rely on imprecise motion estimation or indirect assessments of arterial wall motion.

Recent advances in image processing methodologies using phase-sensitive speckle tracking have led to the

development of elasticity imaging procedures that may be able to overcome the limitations of current imaging modalities in measuring vascular compliance with high resolution. These elasticity imaging methods have the potential to measure intramural wall strain directly using high-resolution ultrasound speckle tracking, without having to rely on lower precision geometric estimates of wall motion to infer strain (12,13). In the clinical setting, elasticity imaging has shown potential to distinguish normal from fibrotic/inelastic vessels (14). It is clear that vascular compliance measurements may help in the evaluation of stenotic vascular lesions as it is recognized that changes in vascular wall elastin and extracellular matrix composition of the media is one of the causes of arterial stiffness (15–17). With this in mind, we are evaluating tools that may allow detailed assessment of vascular mechanics. These image processing tools may allow detailed local vascular lesion characterization, and potentially predict response to local treatment measures such as angioplasty. For example, in order for angioplasty to be successful, the lesion wall architecture must be disrupted and heal in a new geometric configuration with a larger diameter. If a vessel wall is elastic, the intramural architecture will stretch and recoil after the balloon is deflated and withdrawn. In support of this hypothesis, we present the high-resolution ultrasound elasticity data and images generated from normal and stenotic regions of autogenous dialysis fistulae from two subjects prior to undergoing angioplasty.

Address correspondence to: William F. Weitzel, MD, Division of Nephrology, Department of Internal Medicine, University of Michigan Health System, 312 Simpson Memorial Institute, 102 Observatory Road, Ann Arbor, MI 48109 5725, or e-mail: weitzel@umich.edu.

Seminars in Dialysis—Vol 22, No 1 (January–February) 2009
pp. 84–89

DOI: 10.1111/j.1525-139X.2008.00502.x

© 2008 Copyright the Authors.

Journal compilation © 2008 Wiley Periodicals, Inc.

Material and Methods

Elasticity Imaging Procedure

We employed a local, high-resolution ultrasound elasticity imaging method using a linear array ultrasound transducer, with continuous freehand monitoring over the regions of interest (ROI) in the dialysis fistula of the subjects studied. The access vein fistula pulsates in response to the transmitted transmural pulse pressure within the access. A 7-MHz center frequency linear array transducer was used on the surface of the arm over the ROI in the fistulae. Three images were obtained for each subject: (i) near the distal arterial anastomosis, (ii) the stenotic region identified in the fistula, and (iii) the out-flow vein segment downstream from the stenosis. A Philips (Bothell, WA, USA) IU22 was used for data collection at frame rates of approximately 180 frames per second while collecting ultrasound data frame by frame as the investigators viewed the B-scan images. Real-time radio frequency (RF) data collected during imaging were stored and processed off-line.

High resolution can be obtained using RF ultrasound signal containing speckle information that can be used to accurately track the motion of structures within the object imaged (18,19). The first step in elasticity imaging is to estimate the motion between two (not necessarily sequential) frames. Figure 1 illustrates the location “lag” calculated accurately using the characteristic underlying RF signature to estimate the motion of each region with high resolution and

precision within the ultrasound image of the cross section of the vessel. Frame-to-frame displacements are estimated using a two-dimensional correlation-based phase-sensitive speckle tracking technique (20). This particular technique combines the ability of correlation-based algorithms to track relatively large internal displacements with the precision of phase-sensitive methods. First, frame-to-frame lateral and axial displacements are estimated from the position of the maximum correlation coefficient, where a correlation kernel approximately equaling the speckle spot (0.2 mm) is used for optimal strain estimation. The axial displacement estimate is then further refined by determining the zero-crossing position of the phase of the analytic signal correlation. Frame-to-frame displacement error is also reduced using a weighted correlation sum and by filtering spatially adjacent correlation functions prior to displacement estimation (20). A spatial filter twice as large as the kernel size was used to enhance signal-to-noise ratio with good spatial resolution. Frame-to-frame displacement estimates were integrated from and registered to the initial coordinate system (i.e., Lagrangian presentation). All strain measurements were axial measurements, i.e., taken along the ultrasound beam where resolution is greatest. Spatial derivatives of the displacements were thereby computed in the vessel wall in line with top wall or orthogonal to side wall, in order to estimate the radial normal strain (i.e., the radial derivative of the radial displacement).

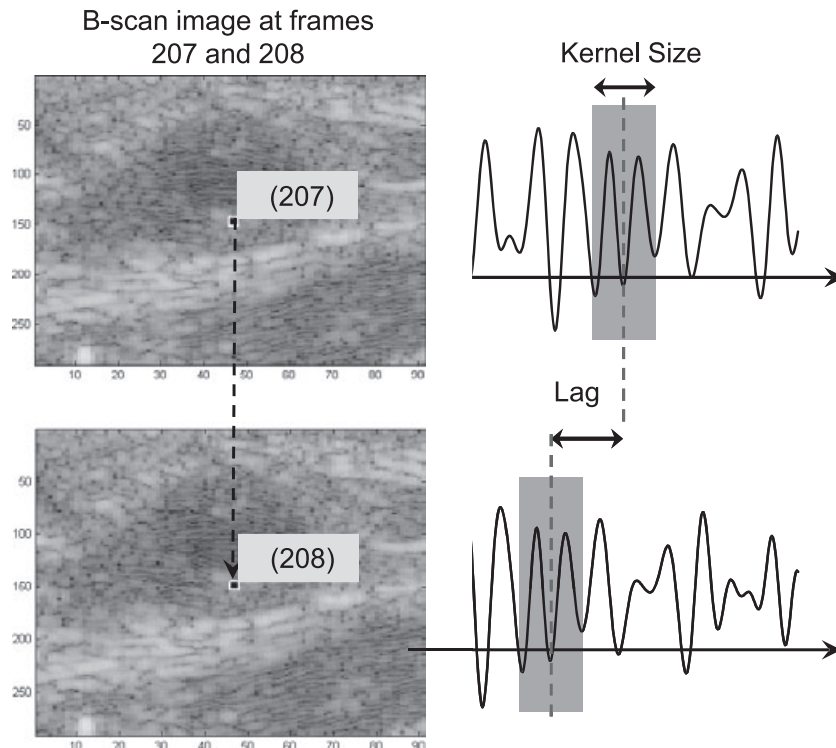


FIG. 1. Illustration of the displacement determined from the frame-to-frame lag distance calculated using the correlation between the characteristic underlying radio-frequency ultrasound signal between frames. Lateral and axial displacements from frame to frame were estimated using correlation-based algorithms and phase-sensitive speckle tracking. Displacement is estimated from the position of the maximum correlation coefficient. A correlation kernel approximately the size of the speckle spot (0.2 mm) is used for optimal strain estimation.

Subjects Studied

After IRB approval two subjects with native vein dialysis fistulae were enrolled for ultrasound elasticity imaging prior to receiving angiography to evaluate fistula dysfunction. Subject 1 was a 61-year-old man with ESRD from diabetes with a left upper extremity cephalic vein fistula. He was referred for fistulogram for elevated venous access pressures. Subject 2 was a 78-year-old man with ESRD from hypertension and nephrectomy for renal cell carcinoma with a left upper arm transposed basilic vein fistula referred for fistulogram for elevated venous access pressures and prolonged bleeding after dialysis.

Results

Elasticity Imaging Results

The accumulated displacement of the fistula wall of each subject was measured relative to the original frame starting at diastole of the cardiac cycle. Using frame-to-frame images of the correlation coefficient produced by speckle tracking, the lumen surface could be easily identified. Consequently, these points were clearly within the intima-media complex. The pixel-by-pixel displacement within the fistula (vein) wall was measured resulting from the cyclic displacement by the pulse pressure. Based on the displacement information, normal accumulated strain values were estimated from direct high-resolution intramural speckle tracking measurements from five ROIs.

Summary of Strain Measurements

As can be seen in Table 1 and Fig. 2, the absolute values of strain are different for normal and stenotic regions. The mean strain of the stenotic ROI on the left side of the wall in subject 1 is 0.98%, but the mean values are three to four times larger in the normal ROI. At the top of the fistula wall in this subject,

TABLE 1. Wall strain measurements (n = 5); local region

	Subject	Region	Mean (%)	STD (%)
Side of wall ^a	1	Normal 1	3.34	1.98
		Normal 2	4.36	1.99
		Stenosis	0.98	1.20
	2	Normal 1	2.34	0.96
		Normal 2	1.86	0.40
		Stenosis	0.52	0.13
Top of wall ^b	1	Normal 1	-1.96	0.40
		Normal 2	-0.90	0.26
		Stenosis	-0.32	0.23
	2	Normal 1	-1.70	0.64
		Normal 2	-1.80	1.05
		Stenosis	-1.04	0.51

^aAll values obtained from the left-hand side of the fistula wall, except that the Normal 1 measurements for subject 2 are from the right-hand side because the left-hand side of the wall was merged with another vessel.

^bAll values obtained from the top of the fistula wall, except Normal 2 in subject 2, which gives values from the bottom of the wall because depth of image at the top was insufficient to calculate strain.

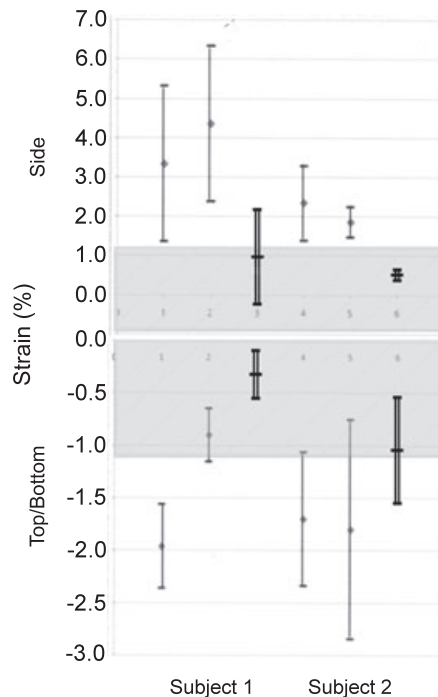


FIG. 2. Comparison of strain values (mean and standard deviation, from Table 1) at normal (single lines) and stenotic (double lines) regions of vessel walls in subjects 1 and 2. The shaded region shows strain values in the stenotic region, which are generally within 1%. The lower values of strain in stenotic regions correspond to increased stiffness.

the mean values are three to six times larger for normal regions than stenotic (0.32%). The absolute values of mean strain are within 1% for stenosis but greater than 1% for normal fistula. The much lower values of strain in regions with stenosis indicate that these regions are correspondingly stiffer than normal fistula. It should be noted that as a reference measurement, wall-strain measurements using the same method in a previous study (13) have shown that under physiologic conditions brachial artery strain measurements in healthy subjects are in the range of 5% ($\pm 2.8\%$ SD), whereas subjects with known vascular disease exhibit stiffer vasculature, with strain measurements in the range of 2.2% ($\pm 0.5\%$ SD).

Figure 3 shows the B-scan and the strain images of the fistula walls in subjects 1 and 2. The dark and white regions show negative and positive strain, respectively. As can be seen in this figure, strain is negative in the approximate region of the fistula wall (see arrow). This negative strain is the result of contraction of the wall during the diastole. The compliance depends on the degree of darkness. Overall, the stenotic region produces smaller strain than normal fistula.

Figure 4 shows the average strain values of the five ROIs for normal and stenotic regions of fistula wall. The ROIs were chosen on the basis of the correlation and strain image. The strain value was -1.7% for normal fistula and -0.32% for stenotic fistula. Thus, the absolute strain value is much smaller for stenotic regions. The approximate size of the ROI box was determined by

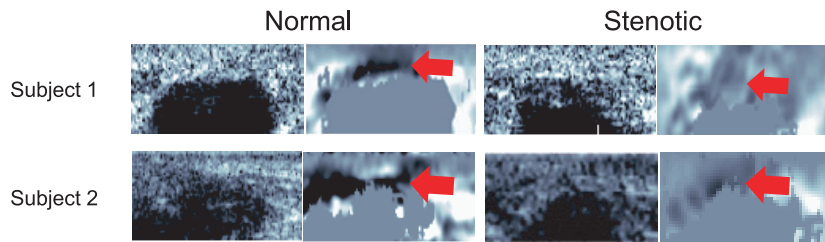


FIG. 3. B-scan and strain images (left-hand and right-hand sides, respectively, of each panel) of normal and stenotic regions of fistula wall in subjects 1 and 2. Degree of darkness in the strain images corresponds to degree of strain. Arrows point to approximate region of fistula wall where strain is negative.

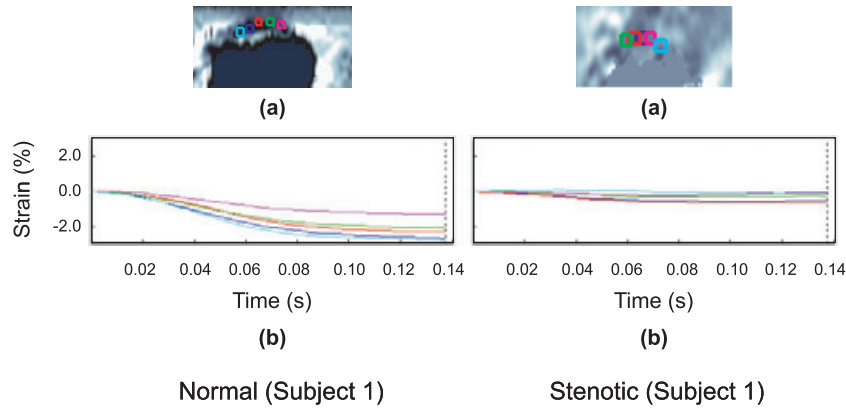


FIG. 4. Strain values from five regions of interest (ROIs) in normal and stenotic regions of fistula wall in subject 1. The ROIs are shown in the strain images (a) as colored boxes, and the strain values of these regions are depicted graphically as a function of time (b). The average of the absolute strain in regions of normal fistula was $1.96 \pm 0.40\%$ compared with $0.32 \pm 0.23\%$ in regions of stenosis. The approximate size of the ROIs is 0.2×0.2 cm. This size is calculated by using the width of the transducer (approximately 5 cm) and the number of pixels inside the ROI box relative to that inside the whole image.

comparing the number of pixels in the box to that of the whole image.

Clinical and Angiographic Results

A summary of the angiogram findings are depicted in Fig. 5 of the stenotic regions with surrounding normal vein segments for subjects 1 and 2, pre and postangioplasty. Subject 1 responded to angioplasty with 8-mm-diameter balloon dilation. Subject 2 initially exhibited elastic recoil after 8-mm balloon dilation but then underwent angioplasty of an upstream arterial lesion in combination with repeat 8-mm balloon angioplasty, and the lesion responded.

Discussion

It is too early to draw firm conclusions about the role ultrasound phase-sensitive speckle tracking may play in managing dialysis vascular access. Nevertheless, these preliminary results do show the potential utility for this novel imaging tool to provide high-resolution strain estimates that may accurately reflect vascular mechanical properties. These mechanical properties, being related to the cellular and extracellular matrix molecular structure of stenotic lesions, may be able to predict lesion response to mechanical treatments such as angioplasty. For strain

to be measured, an underlying stress must be applied to the vessel wall. For this feasibility study we observed the strain produced by the stress provided by the underlying physiologic pulse pressure. Given that this stress is variable, being dependent on patient blood pressure and pressure gradients along the vascular access, this

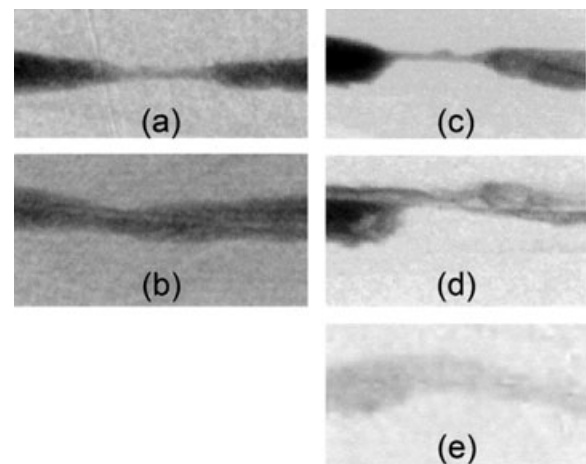


FIG. 5. Preangioplasty images of stenotic regions in subjects 1 and 2 (a and c, respectively). Subject 1 responded to angioplasty with 8-mm balloon dilation (b), whereas subject 2 experienced elastic recoil (d) and then responded to repeat angioplasty (e).

measurement method will undoubtedly require standardization of the deformational stress (blood pressure) to provide more accurate comparisons between patients in the future. Standardization methods have been explored using these imaging procedures in transplant kidneys (21) and brachial artery elasticity (14).

The diagnostic sensitivity of vascular strain imaging may be greatly increased by exploring the nonlinear behavior of the vascular stress-strain relationship (14). Under conditions of normal physiologic loading, the mean vessel pressure within the dialysis access is normally less than half the mean arterial pressure (22) and lower in fistulas than grafts. When elevated in the presence of an outflow stenosis, this pressure decreases in response to correcting the outflow lesion (23). As pressure increases, because of the nonlinear properties of the vessel wall (24,25), there is a higher effective elastic modulus in the wall that will tend to diminish the pulse pressure-induced strain. Therefore, the diagnostic range of the method we used may be increased in the future by using a pressure-equalization method that we are currently evaluating (12,14). In addition, the dampened pressure in the segment of the fistula downstream from the stenosis will tend to diminish the wall deformation and strain even in the setting of a compliant vascular wall. Understanding these limitations, the findings in this first feasibility study demonstrate the potential for high sensitivity of this method for detection of local regions of greater and lesser vascular compliance. We also observe that these findings are compatible with our previous study results showing the method may distinguish normal from diseased arteries in vivo (14).

An important distinction should be made between the high-resolution method we used and previous measurements of vessel elasticity over a range of differential wall pressures (26,27). Prior studies have made important contributions to our understanding of vessel compliance using results inferred from geometric changes such as artery diameter and lumen cross section based on a numerical Langewouters model (28). The precision of the speckle tracking technique we used offers the possibility of detecting subtle underlying structural changes within the vascular wall and measuring the corresponding intramural changes in elastic properties with unprecedented resolution, precision, and accuracy down to tens of microns depending on the ultrasound frequency used.

While at present this method is computationally time intensive, recent advances suggest that it may be useful for expanded research applications and ultimately as an adjunct to conventional imaging to guide therapy. For example, stenotic lesions fail to respond to conventional angioplasty and may require additional mechanical interventions such as stents (29,30) or cutting balloons (31). High-resolution measurement of the vascular mechanics of stenotic lesions may improve individualized prediction of lesion responsiveness to angioplasty and guide decision making. The dialysis access elastograms of the stenotic lesions obtained from our two subjects with native fistulas prior to angioplasty showed the lesions to be more rigid than normal regions of the fistula. In addition, different regions of the vessel wall showed different elastic properties with strain imaging,

some regions with greater variation in intra-lesion strain measurements and greater compliance than the other less compliant regions of the stenosis. Further study will be required to determine whether these highly accurate, high-resolution images will allow treatment individualization.

In summary, the clinical appeal of this technology for patients focuses on an improved noninvasive imaging method that can give high-resolution structural and geometric information about the anatomy and mechanical properties of the fistula and stenosis. Although the current method allows only computationally time-intensive research measurements to be performed off-line, newer methods that can be used in real-time or near real-time are being developed that will be suitable for more widespread clinical evaluation. This novel method of measuring the mechanical properties of local vein/fistula remodeling with high resolution may have great potential for tracking vein remodeling, predicting stenosis development, and guiding future treatment decisions.

Acknowledgments

The authors thank Philips Ultrasound for assistance with RF data capture. This work was supported in part by NIH Grant DK-62848 and a grant from the Renal Research Institute.

References

1. Bonnefous O, Montaudon M, Sananes JC, Denis E: Non invasive echographic techniques for vessel wall characterization. *IEEE Ultrason Symp Proc* 2:1059-1064, 1996
2. Taniwaki H, Shoji T, Emoto M, Kawagishi T, Ishimura E, Inaba M, Okuno Y, Nishizawa Y: Femoral artery wall thickness and stiffness in evaluation of peripheral vascular disease in type 2 diabetes mellitus. *Atherosclerosis* 158:207-214, 2001
3. Luik AJ, Spek JJ, Charra B, van Bortel LMAB, Laurent G, Leunissen KML: Vessel compliance in patients on long-treatment-time dialysis. *Nephrol Dial Transplant* 12:2629-2632, 1997
4. Guérin A, London G, Marchais S, Metivier F: Vessel stiffening and vascular calcifications in end-stage renal disease. *Nephrol Dial Transplant* 15:1014-1021, 2000
5. Bonnefous O, Criton A, Germond L, Denis E: New TDI developments for vascular and cardiac applications. *IEEE Ultrason Symp Proc* 2:1285-1290, 2000
6. Eriksson A, Greiff E, Loupas T, Persson M, Pesque P: Vessel pulse wave velocity with tissue Doppler imaging. *Ultrasound Med Biol* 28:571-580, 2002
7. Persson M, Eriksson A, Persson HW, Lindstrom K: Estimation of arterial pulse wave velocity with a new improved tissue Doppler method. *Proc 23rd Annu EMBS Int Conf* 1:188-191, 2001
8. Mai JJ, Insana MF: Vascular strain imaging of internal deformation. *Ultrasound Med Biol* 28:1475-1484, 2002
9. Duprez D, de Buyzere M, van den Noortgat N, Simoons J, Achten E, Clement D, Afschrift M, Cohn J: Relationship between periventricular or deep white matter lesions and vessel elasticity indices in very old people. *Age Ageing* 30:325-330, 2001
10. Blacher J, Guerin A, Pannier B, Marchais S, Safar M, London G: Impact of aortic stiffness on survival in end-stage renal disease. *Circulation* 99:2434-2439, 1999
11. Blacher J, Pannier B, Guerin A, Marchais S, Safar M, London G: Carotid vessel stiffness as a predictor of cardiovascular and all-cause mortality in end-stage renal disease. *Hypertension* 32:570-574, 1998
12. Kim K, Weitzel WF, Xie H, Rubin JM, Jia C, O'Donnell M: Dual arterial elastic modulus reconstruction from *in-vivo* strain imaging and PWV. *IEEE Int Ultrason Symp Proc* 381-384, 2005
13. Kim K, Weitzel WF, Rubin JM, Xie H, Chen X, O'Donnell M: Vascular intramural strain imaging using arterial pressure equalization. *Ultrasound Med Biol* 30:761-771, 2004

14. Weitzel WF, Kim K, Rubin JM, Xie H, O'Donnell M: Renal advances in ultrasound elasticity imaging: Measuring the compliance of arteries and kidneys in end-stage renal disease. *Blood Purif* 23:10–17, 2005
15. Faury G: Function–structure relationship of elastic arteries in evolution: from microfibrils to elastin and elastic fibres. *Pathol Biol (Paris)* 49:310–325, 2001
16. Bilato C, Crow MT: Atherosclerosis and the vascular biology of aging. *Aging (Milano)* 8:221–234, 1996
17. Bruel A, Oxlund H: Changes in biomechanical properties, composition of collagen and elastin, and advanced glycation endproducts of the rat aorta in relation to age. *Atherosclerosis* 127:155–165, 1996
18. Emelianov SY, Erkamp RQ, Lubinski MA, Skovoroda AR, O'Donnell M: Non-linear tissue elasticity: adaptive elasticity imaging for large deformations. *IEEE Ultrason Symp Proc* 2:1753–1756, 1998
19. O'Donnell M, Skovoroda AR, Shapo BM, Emelianov SY: Internal displacement and strain imaging using ultrasonic speckle tracking. *IEEE Trans Ultrason Ferroelectr Freq Control* 41:314–325, 1994
20. Lubinski MA, Emelianov SY, O'Donnell M: Speckle tracking methods for ultrasonic elasticity imaging using short time correlation. *IEEE Trans Ultrason Ferroelectr Freq Control* 46:82–96, 1999
21. Weitzel WF, Kim K, Rubin JM, Wiggins RC, Xie H, Chen X, Emelianov SY, O'Donnell M: Feasibility of applying ultrasound strain imaging to detect renal transplant chronic allograft nephropathy. *Kidney Int* 65:733–736, 2004
22. Besarab A, Dinwiddie L: Changes noted to KDOQI guidelines for vascular access. *Nephrol News Issues* 20:36, 2006
23. Asif A, Besarab A, Gadalean F, Merrill D, Rismeyer AE, Contreras G, Leclercq B, Lenz O, Wallach J, Wallach J, Levine MI: Utility of static pressure ratio recording during angioplasty of arteriovenous graft stenosis. *Semin Dial* 19:551–556, 2006
24. Bergel DH: The static elastic properties of the vessel wall. *J Physiol* 156:445–457, 1961
25. Bergel DH: The dynamic elastic properties of the vessel wall. *J Physiol* 156:458–469, 1961
26. Bank AJ, Kaiser DR, Rajala S, Marchais S, Cheng A: In vivo human brachial artery elastic mechanics effects of smooth muscle relaxation. *Circulation* 100:41–47, 1999
27. Kaiser DR, Mullen K, Bank AJ: Brachial artery elastic mechanics in patients with heart failure. *Hypertension* 38:1440–1445, 2001
28. Langewouters GJ, Wesseling KH, Goedhard WJA: The static elastic properties of 45 human thoracic and 20 abdominal aortas in vitro and the parameters of a new model. *J Biomech* 17:425–435, 1984
29. Vogel PM, Parise C: SMART stent for salvage of hemodialysis access grafts. *J Vasc Interv Radiol* 15:1051–1060, 2004
30. Sreenarasimhaiah VP, Margassery SK, Martin KJ, Bander SJ: Salvage of thrombosed dialysis access grafts with venous anastomosis stents. *Kidney Int* 67:678–684, 2005
31. Singer-Jordan J, Papura S: Cutting balloon angioplasty for primary treatment of hemodialysis fistula venous stenoses: preliminary results. *J Vasc Interv Radiol* 16:25–29, 2005